IEICE TRANS. ELECTRON., VOL.E106–C, NO.11 NOVEMBER 2023

INVITED PAPER *Joint Special Section on Opto-electronics and Communications for Future Optical Network*

128 Gbit/s Operation of AXEL with Energy Efficiency of 1.5 pJ/bit for Optical Interconnection

Wataru KOBAYASHI[†a)], **Shigeru KANAZAWA**[††], **Takahiko SHINDO**[†], **Manabu MITSUHARA**[†], ***and*** **Fumito NAKAJIMA**[†], ***Members***

SUMMARY We evaluated the energy efficiency per 1-bit transmission of an optical light source on InP substrate to achieve optical interconnection. A semiconductor optical amplifier (SOA) assisted extended reach EADFB laser (AXEL) was utilized as the optical light source to enhance the energy efficiency compared to the conventional electro-absorption modulator integrated with a DFB laser (EML). The AXEL has frequency bandwidth extendibility for operation of over 100 Gbit/s, which is difficult when using a vertical cavity surface emitting laser (VCSEL) without an equalizer. By designing the AXEL for low power consumption, we were able to achieve 64-Gbit/s, 1.0 pJ/bit and 128-Gbit/s, 1.5 pJ/bit operation at 50°C with the transmitter dispersion and eye closure quaternary of 1.1 dB.

key words: *electro-absorption modulator, semiconductor optical amplifier, DFB laser, pulse amplitude modulation*

1. Introduction

Cyber-physical systems (CPS) based on Internet of Things (IoT) sensor networks are increasingly being utilized to achieve the Society 5.0 concept, where remotely driven sensors generate huge data. This has led to an increase of the global data sphere at the rate of about 30% per year [1]. The generated data need to be transmitted to a processor such as an edge computer or a cloud computer, and this requires the network system to continuously expand its transmission capacity while at the same time reducing power consumption. The total power consumption of data centers worldwide is predicted to increase dramatically from approximately 200 TWh in 2018 to 3000 TWh by 2030 [2]. The bulk of this enormous amount of power is taken up by IT equipment, whose ratio is defined by a power usage effectiveness (PUE). Generally, IT equipment consumes more than half of the power in a data center, so for this reason, reducing the power consumption of IT equipment can be viewed as a vital social issue to maintain a sustainable society.

Against this background, IT equipment such as optical light sources need to enhance their energy efficiency per 1 bit of transmission. Various standardizations are in place for the optical light source of an optical network system, including those put forth by the IEEE [3], [4] and the Consortium for On-Board Optics (COBO) [5], along with Peripheral Component Interconnect Express (PCIe). According to the PCIe specification, the signaling rate doubles as its technology generation increases: e.g., 16 Gbit/s for PCIe 4.0 and 32 Gbit/s for PCIe 5.0. One report has indicated that optical interconnect can dramatically reduce power consumption compared to electrical interconnection as the signaling rate increases to high speeds such as 64 Gbit/s (PCIe 6.0) and 128 Gbit/s (PCIe 7.0) [6] because the electrical transmission loss of an electrical interconnection increases as the signaling rate increases. This means an optical light source that features both high-speed operation (over 64 Gbit/s) and high energy efficiency will be an attractive candidate for optical interconnection applications.

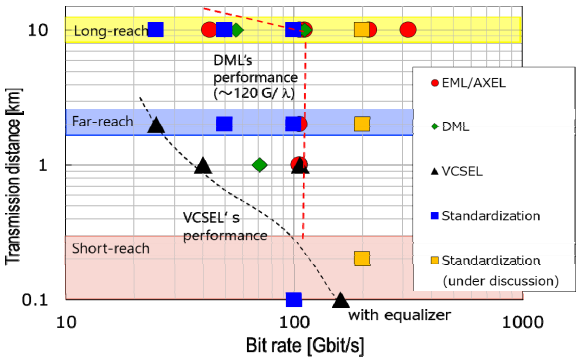

Fig. 1 Comparison of light sources from bit rate and transmission distance viewpoints.

The main candidates for an optical source that can be driven over 64 Gbit/s are compared in Fig. 1. The EML has the largest frequency bandwidth compared to the VCSEL and the directly modulated laser (DML), while from the viewpoint of low power consumption, the VCSEL is superior to the DML and EML for operations up to 25 Gbit/s. However, if the signaling rate is higher than 64 Gbit/s, the VCSEL requires an equalizer to compensate for its frequency bandwidth shortage, as its general frequency bandwidth is about 25 GHz [7]. This means it requires a power consumption increase to reach the same level as the DML and EML.

In light of the above background, the main challenge with the optical light source is how to improve the energy efficiency per 1-bit transmission. The main point to keep in mind here is that if a signaling rate increases with the

Manuscript received December 27, 2022.
Manuscript revised April 7, 2023.
Manuscript publicized June 5, 2023.
[†]The authors are with NTT Device Technology Laboratories, NTT Corporation, Atsugi-shi, 243–0198 Japan.
[††]The author is with NTT Device Innovation Center, NTT Corporation, Atsugi-shi, 243–0198 Japan.
a) E-mail: wataru.kobayashi.xw@hco.ntt.co.jp
DOI: 10.1587/transele.2022OCI0002

same power consumption, the energy efficiency will also increase. In principle, the frequency bandwidth of the EML is larger than that of the DML and VCSEL, so the EML has an advantage in operations over 64 Gbit/s. Therefore, as the signaling rate gets higher, the energy efficiency of the EML will be superior to the other candidates. We recently proposed an approach based on an SOA-assisted extended-reach EADFB laser (AXEL) to improve the EML energy efficiency [8], [9] and were able to almost double the energy efficiency with the same optical output. By using the AXEL, we realized the energy efficiency of less than 1.5 pJ/bit at 64 and 128 Gbit/s [10]. But the fine-tuning method for increasing the energy efficiency with the AXEL is not sufficiently described.

In this paper, we fine-tune the AXEL to improve the energy efficiency at a signaling rate of over 64 Gbit/s and 128 Gbit/s. We investigate the optimal driving condition for the AXEL by comparing a simulation and an experiment.

2. Concept

Our concept is to enhance the energy efficiency per 1-bit transmission. In our prior work, we reported an EML with the power consumption of about 180 mW at 40 Gbit/s and the corresponding energy efficiency of about 4.5 pJ/bit [11]. By using the SOA to reduce the power consumption of the EML, we could reduce the power consumption to 140 mW and the corresponding energy efficiency to about 3.5 pJ/bit.

However, since optical interconnection requires the same level of energy efficiency as the VCSEL in a 25-Gbit/s optical system, we need to further reduce the power consumption and improve the energy efficiency to be in the 1.0- to 2.0-pJ/bit range.

We utilize two approaches to achieve this target. The first is to increase the operating speed so as to increase the denominator of the energy efficiency. This approach is suitable for the AXEL because an EA modulator (EAM) has a large extendibility of high-speed operation [12].

The second approach is to carefully design the DFB laser and SOA section, as these sections can be implemented with a reduced injection current to the DFB laser (I_{LD}) and SOA section (I_{SOA}). Our overall concept is shown in Fig. 2. Generally, an EML requires a high output power from the DFB laser section to compensate for the optical loss of the EAM, and this results in a deterioration of the energy efficiency. In contrast, the SOA section is free from the optical loss of the EAM due to its spatial configuration, which allows us to reduce the I_{LD} while increasing the I_{SOA} with the same optical output. This approach enhances the energy efficiency of the AXEL compared to the EML.

In our prior work, we focused on instilling the AXEL with a high output power for NG-PON applications [13]. In the current work, we focus on the energy efficiency.

3. Design Methodology

First, we determined the operating condition for the AXEL to evaluate the energy efficiency per 1-bit transmission of the optical light source. When looking at the entire power consumption of the optical light source, we need to take into account the thermo-electric cooler (TEC) and the driver of the EAM. To reduce the power consumption of the TEC, we set the operating temperature to 50°C, as this temperature can reduce the power consumption with a semi-cooled operation. This semi-cooled operation can minimize the power consumption of TEC, because the power consumption of TEC depends on the temperature difference between a case temperature and a setting temperature of TEC [14]. We also evaluated the device characteristics at 80°C to determine the extendibility of TEC-free operation. The power consumption in the EAM driver depends on the required modulation voltage swing (V_{pp}) for the EAM, so from a practical viewpoint, we set the V_{pp} to below 1.5 V, as the general V_{pp} of an EAM driver is less than 1.5 V.

Next, we evaluated the energy efficiency at the determined operating condition of 50°C. To determine the optimum I_{LD} and I_{SOA}, we evaluated the optical output power using a simulation and an experiment. First, we calculated the light-current (L-I) characteristics for the LD section by using LASTIP (Crosslight Inc.) [15]. Figure 3 shows the calculated output power of a DFB laser with a 300-μm cavity length at 50°C. The simulation also included the optical coupling loss to an optical fiber and the optical loss of the EAM. As shown, when I_{LD} increased from 40 to 60 mA, the optical output power increased from 5.9 to 8.1 mW, which corresponds to an optical gain of about 1.3 dB.

To clarify the optimum condition of I_{LD} and I_{SOA}, we also calculated the optical gain with various I_{SOA}. Figure 4

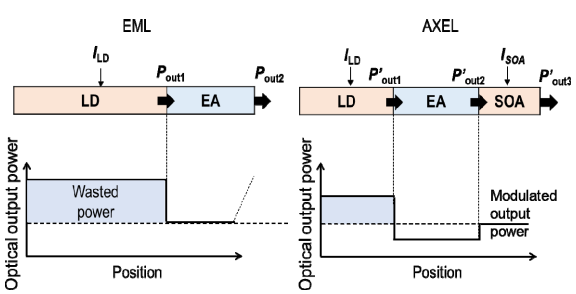

Fig. 2 Concept of this work.

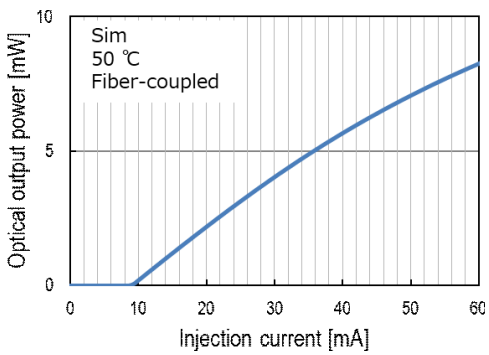

Fig. 3 Calculated L-I characteristics of DFB laser.

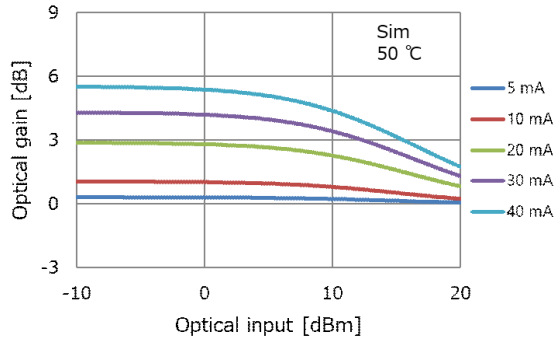

Fig. 4 Calculated optical gain vs. input optical power.

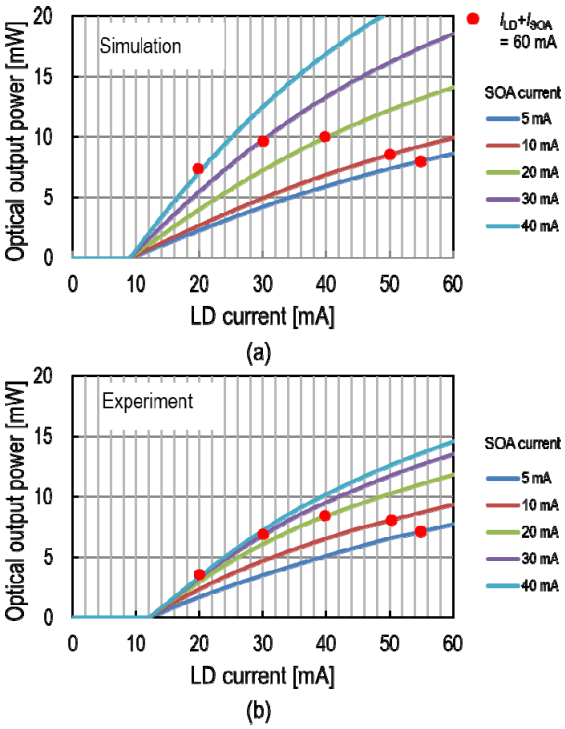

Fig. 5 L-I characteristics of AXEL: (a) simulation and (b) experiment.

shows the calculated optical gain versus optical input for the SOA length of 100 µm at 50°C. This calculation was done using the rate equation detailed in [11]. As shown, as I_{SOA} increased from 0 to 20 mA, the optical gain increased by 3 dB. This value is larger than the gain difference of the DFB laser with the I_{LD} of 40 to 60 mA. These simulation results demonstrate that the AXEL can improve the energy efficiency of the EML.

Next, we utilized the L-I characteristics and SOA gain characteristics shown in Figs. 3 and 4 to evaluate the optical output power of the AXEL. Figure 5 shows the L-I characteristics of the AXEL used for the simulation and experiment at 50°C. The red circles indicate the data whose sum of I_{LD} and I_{SOA} was 60 mA. As we can see, the optimum conditions of I_{LD} and I_{SOA} were about 40 mA and 20 mA when the length of the LD and SOA were 300 and 100 µm, respectively. Although the output power in the experiment

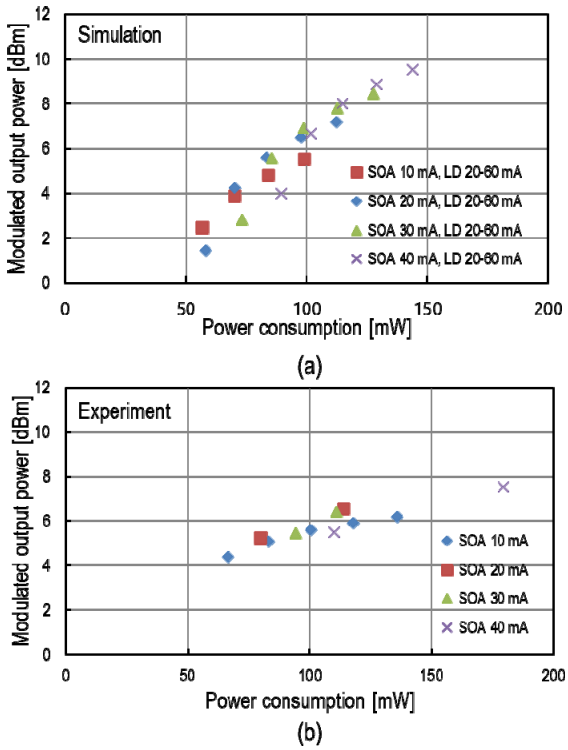

Fig. 6 Relationship between power consumption and modulated output power at 50°C.

was smaller than that in the simulation, the tendency of the input current versus optical output was similar. These results clarify the optimum condition for providing the maximum optical output.

Next, we evaluated the power consumption and modulated output power at 50°C. To evaluate the entire power consumption of the AXEL chip, we assumed the power consumption of the EAM to be 12 mW and the typical values of the DC bias voltage and photo current of the EA section to be −1.2 V and 10 mA, respectively. For the simulation, we assumed the EAM optical loss of 5 dB and depicted the sum of the power consumption for the LD, EAM, and SOA section on the vertical axis, where the vertical axis increases as the I_{LD} increases. When we consider the energy efficiency of 1.0 pJ/bit, the allocated power consumption was 64 mW for 64-Gbit/s operation and 128 mW for 128-Gbit/s operation. As shown in Fig. 6, we could achieve the modulated output power of about 5 dBm and 7 dBm when the power consumption of the AXEL was 60 mW and 128 mW, respectively. Although the maximum optical out power for 1.0 pJ/bit at 64 Gbit/s operation was limited to 5 dBm, we could control the power consumption by reducing the optical output power. In this work, the optical output power was set to a sufficiently high level to evaluate modulation characteristics such as eye diagram and eye closure quaternary (TDECQ) (discussed later).

To investigate the extendibility of the TEC-free operation of the AXEL, we also measured the temperature dependence of the modulated output power at 80°C. Fig-

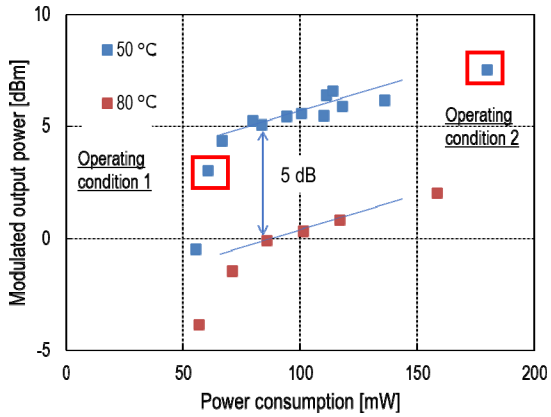

Fig. 7 Temperature dependence of modulated output power vs. power consumption.

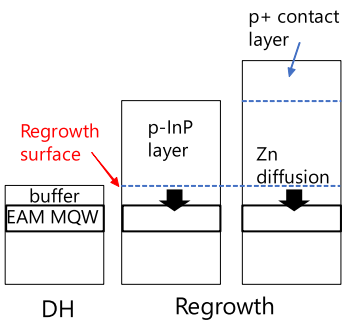

Fig. 8 Epitaxial layer of the sample.

ure 7 shows the power consumption versus modulated output power. As we can see, the modulated output power decreased by 5 dB when the temperature increased by 30°C. However, since the AXEL could suppress the optical loss of the EAM, it was able to provide the modulated output power of over 0 dBm when the power consumption was about 80 mW. These results indicate that 1.0-pJ/bit operation with the modulated output power of over 0 dBm can be achieved when the signaling rate is over 80 Gbit/s. Note that the red square in Fig. 7 indicates the experimental conditions for measuring the modulation characteristics shown later in Figs. 12 and 16.

Next, we fine-tuned the EAM design to increase the energy efficiency per 1-bit transmission. Generally, the EAM has a trade-off relationship between the frequency bandwidth and extinction ratio (ER). To enhance the frequency bandwidth, we need to reduce the parasitic capacitance and therefore shorten the EAM, but on the other hand, the optical network system requires a high enough ER to achieve sufficient bit error rate (BER) characteristics, and therefore we need a long EAM. To ease this trade-off, we need to enhance the ER per EAM unit length. The impurity concentration of the EAM epitaxial layer is the main issue here, specifically, the diffusion of zinc (Zn) from the cladding layer [16]. We therefore evaluated the Zn concentration in the EAM section using the three epitaxial layer structures shown in Fig. 8. The three samples were compared to clarify the influence of

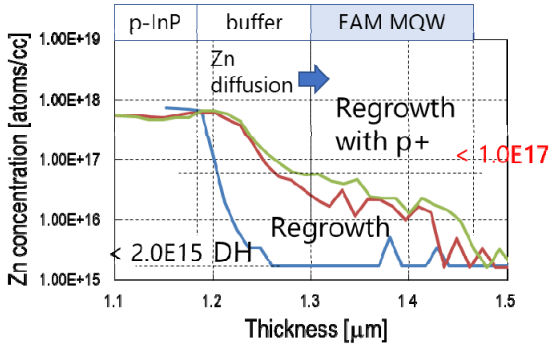

Fig. 9 Zn concentration for the EAM.

Zn diffusion during the epitaxial regrowth process. As the AXEL consists of an LD, EA, and SOA, we inevitably require a regrowth process for the p-cladding layer. Generally, Zn diffusion is caused by a kick-out mechanism [17], [18], where Zn atoms move through vacancies created by group III elements. For this reason, Zn diffusion occurs easily during temperature changes of the epitaxial growth, and it therefore has a severe effect on the epitaxial regrowth process. We consider that the interstitial Zn atom can easily diffuse into the MQW region. In order to suppress the generation of interstitial Zn atom, p+-InGaAs layers were grown at a relatively low substrate temperature.

Figure 9 shows the depth profiles of the secondary ion mass spectrometer (SIMS) signals of Zn in the EAM multiple-quantum-well (MQW) epitaxial layer. As we can see, Zn diffusion was suppressed to less than 2.0E + 15 cm^{-3} without a regrowth process. After optimizing the regrowth process, we were able to obtain the Zn diffusion of less than 1.0E + 17 cm^{-3} at the interfacial layer between the buffer and EAM MQW. Generally, the deterioration of the extinction characteristics can be suppressed if the Zn diffusion is less than 1.0E + 17 cm^{-3} [19]. We optimized the epitaxial growth condition of the p-cladding layer and p+ contact layer.

Next, we utilized the epitaxial regrowth technique described above to fabricate the AXEL. Our main objective was to balance the trade-off relationship between the frequency bandwidth and ER. Figure 10 shows the extinction characteristics of 75- and 125-μm long EAM at 50°C. As we can see, ER reached about 15 dB with the DC bias difference of 1.5 V for 125-μm EAM, while it was about 8 dB for 75-μm EAM. If we operate EAM with pulse amplitude modulation, we need the ER to be over 15 dB, which is why we set the EAM length to 125 μm.

We also measured the frequency bandwidth of EAM. Figure 11 shows the electrical to optical (EO) frequency response for various lengths of EAM at 50°C. As shown in figure, we can achieve the 3-dB-down frequency bandwidth ($f_{3\,dB}$) of over 40 GHz for 125 μm long EAM. The peaking level around 15 GHz was controlled by the bonding wire between a RF circuit board and a termination resistance. By taking consider Figs. 10 and 11, we set the EAM length to 125 μm.

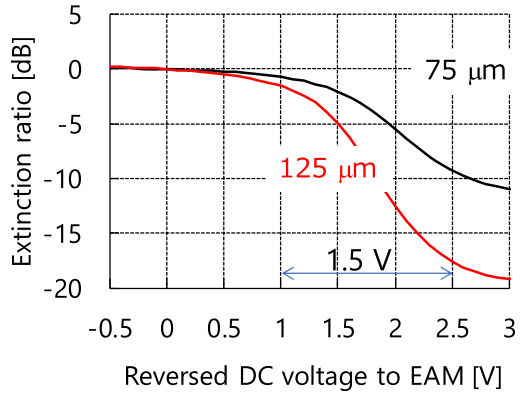

Fig. 10 Extinction characteristics of 75- and 125-µm long EA modulator.

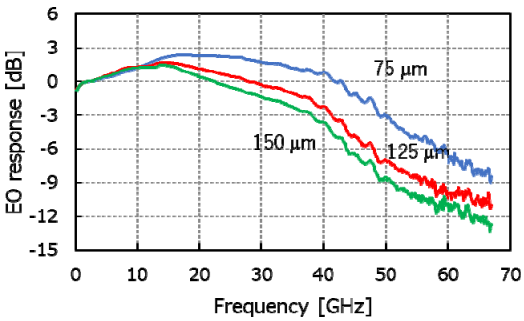

Fig. 11 EO response for various lengths of EAM at 50°C.

4. Device Characteristics

Some of the basic structure of the AXEL we fabricated has already been reported [20]. First, we evaluated the 64-Gbit/s modulation characteristics at 50 and 80°C, where the V_{pp} was set to 1.5 V. The electrical signal input to the device was non-return zero (NRZ) with a pseudorandom binary sequence (PRBS) of $2^{15} - 1$. The applied bias voltage was −1.3 V at 50°C and −0.65 V at 80°C. Figure 12 shows 64-Gbit/s eye diagrams, where we can see that clear eye openings were obtained for each temperature. The dynamic extinction ratios (DERs) were 9.5 dB and 9.7 dB, respectively. The measured optical modulation amplitudes (OMA) were 5.0 and 0.6 dBm. The measured power consumption was 60 and 71 mW and the energy efficiency was 1.0 pJ/bit and 1.2 pJ/bit, respectively. These results indicate that the AXEL can be operated at 1.0 pJ/bit when the signaling rate is 64 Gbit/s, thus making it an attractive candidate for application of PCIe 6.0.

Next, we evaluated the 128-Gbit/s operation to determine whether AXEL is suitable for PCIe 7.0. Figure 13 shows the 64-Gbaud/s pulse amplitude modulation 4 (PAM4) electrical signal that was input to the device. Since the EAM has non-linearity for extinction characteristics, we tuned the bias voltage of each level to compensate.

Figure 14 shows the eye diagrams for the V_{pp} of 0.8, 1.0, and 1.5 V. The measured extinction ratios between levels 0 and 3 were 4.6, 5.9, and 8.0 dB, respectively, and the measured TDECQ values were 1.1, 1.2, and 1.7 dB, respectively. These results demonstrate the importance of compensating for the non-linearity of the EAM to reduce the TDECQ.

Figure 15 shows the PAM4 signals whose bias voltages between levels 0 and 3 (V_{pp}) were 0.8, 1.0, and 1.5 V, respectively. The vertical axis shows optical power from

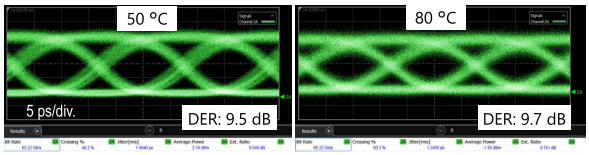

Fig. 12 64-Gbit/s eye diagrams for 50 and 80°C.

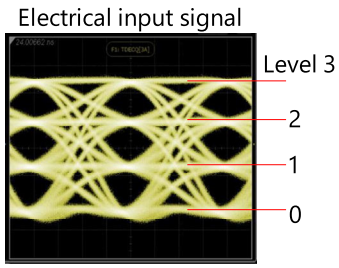

Fig. 13 Electrical input signal to EAM.

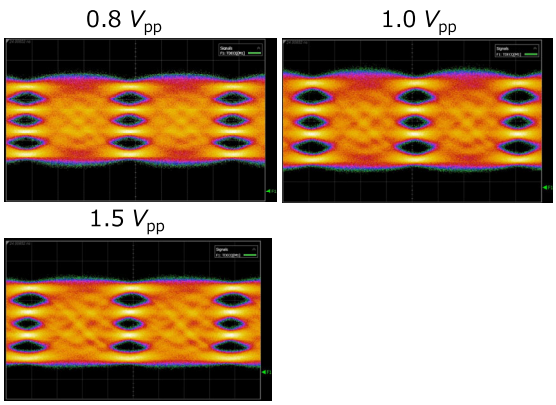

Fig. 14 Eye diagrams for modulation voltage swings of 0.8, 1.0, and 1.5 V_{pp} at 50°C.

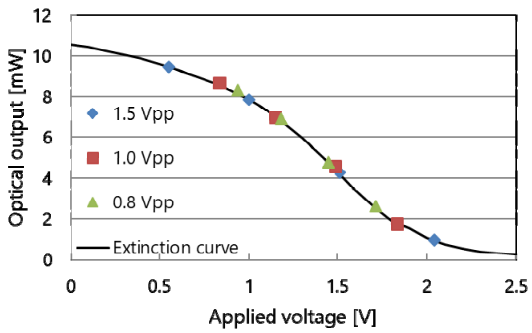

Fig. 15 Extinction characteristics of 125-µm-long EAM.

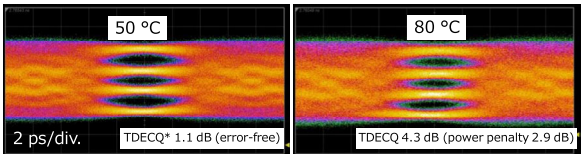

Fig. 16 128-Gbit/s eye diagrams for 50 and 80°C.

the AXEL at 50°C with linear scale. We set each bias voltage to obtain the uniform PAM4 optical eye diagram while compensating for the non-linearity of the extinction characteristics of the EAM.

Finally, we measured the temperature dependence of the eye diagrams. Figure 16 shows 128-Gbit/s eye diagrams for 50 and 80°C, where the modulation voltage swing was set to 0.8 V_{pp}. As we can see, the TDECQ values were 1.1 dB and 4.3 dB, respectively. For the case of 1.1 dB, error-free operation was achieved. The power consumption was 180 and 160 mW, and the corresponding energy efficiency was 1.5 and 1.2 pJ/bit. The measured optical modulation amplitudes were 7.6 and 1.4 dBm. These results demonstrate that the AXEL is an attractive optical source candidate for application of PCIe 7.0.

5. Conclusion

We designed and fabricated a semiconductor assisted extended EADFB laser (AXEL) for use as an optical interconnection. Compared to the roughly 4.5-pJ/bit energy efficiency of a conventional EML, the proposed AXEL achieved 1.0 pJ/bit for 64 Gbit/s and 1.5 pJ/bit for 128 Gbit/s. We clarified the optimum operating current condition of the LD and SOA section through simulations and experiments and also mitigated the tradeoff relationship between ER and the frequency bandwidth of the EAM by fine-tuning its length. To increase the ER per EAM unit length, we focused on suppressing the impurity of the EAM section and optimized the regrowth process of the p-cladding layer and were able to simultaneously achieve the high-speed operation of over 64 Gbit/s and high energy efficiency of 1.5 pJ/bit. These results demonstrate that the AXEL is an attractive candidate for the optical source of optical interconnection applications such as PCIe 6.0 and 7.0.

Acknowledgments

We thank Prof. Hiroshi Yasaka of the Research Institute of Electrical Communication, Tohoku University for his valuable advice. We also thank H. Minami, M. Hosoya, K. Takahashi, and K. Hirai for helpful technical support.

References

[1] Data Age 2025, sponsored by Seagate with data from IDC Global DataSphere, Nov. 2018.
[2] N. Jones, "How to stop data centres from gobbling up the world's electricity," Nature, vol.561, pp.163–166, 2018.
[3] http://www.ieee802.org/3/ba/
[4] http://www.ieee802.org/3/bs/
[5] https://www.onboardoptics.org
[6] Ministry of Economy, Trade and Industry. https://www.meti.go.jp/press/2021/10/20211019002/20211019002-1.pdf
[7] L.M. Giovane, J. Wang, M.V.R. Murty, A.L. Harren, A.-N. Cheng, D. Dolfi, Z.-W. Feng, N. Leong, A. Sridhara, S.-J. Taslim, and J. Chu, "Development of Next Generation Data Communication VCSELs," Optical Fiber Communication Conference (OFC) 2020, M3D.5, San Diego, CA, USA, March, 2020.
[8] W. Kobayashi, N. Fujiwara, T. Shindo, S. Kanazawa, K. Hasebe, H. Ishii, and M. Itoh, "Ultra low power consumption operation of SOA assisted extended reach EADFB laser (AXEL)," Proc. OECC2016, WD3-2, Niigata, Japan 2016.
[9] W. Kobayashi, N. Fujiwara, T. Shindo, Y. Ohiso, S. Kanazawa, H. Ishii, K. Hasebe, H. Matsuzaki, and M. Itoh, "Advantages of SOA assisted extended reach EADFB laser (AXEL) for operation at low power and with extended transmission reach," IEICE Trans. on electronics, vol.E100-C, no.10, pp.759–766, Oct. 2017.
[10] W. Kobayashi, S. Kanazawa, T. Shindo, M. Mitsuhara, and F. Nakajima, "1.5 pJ/bit, 128 Gb/s, 50°C operation of AXEL for short reach application," 27th OptoElectronics and Communications Conference (OECC) and 2022 International Conference on Photonics in Switching and Computing (PSC), WD1-2, Toyama, Japan, July 2022.
[11] W. Kobayashi, M. Arai, T. Fujisawa, T. Sato, T. Ito, K. Hasebe, S. Kanazawa, Y. Ueda, T. Yamanaka, and H. Sanjoh, "Novel approach for chirp and output power compensation applied to a 40-Gbit/s EADFB laser integrated with a short SOA," Optics Express, vol.23, no.7, pp.9533–9542, April, 2015.
[12] S. Kanazawa, H. Yamazaki, Y. Nakanishi, Y. Ueda, W. Kobayashi, Y. Muramoto, H. Ishii, and H. Sanjoh, "214-Gb/s 4-PAM operation of flip-chip interconnection EADFB laser module," IEEE Journal of Lightwave Technology, vol.35, no.3, pp.418–422, Feb. 2017.
[13] T. Shindo, W. Kobayashi, N. Fujiwara, Y. Ohiso, K. Hasebe, H. Ishii, and M. Itoh, "High modulated output power over 9.0 dBm with 1570 nm wavelength SOA assisted extended reach EADFB Laser (AXEL)," IEEE Journal of Selected Topics of Quantum Electronics in Semiconductor Lasers, vol.23, no.6, 1500607, Nov./Dec. 2017.
[14] N. Okada, T. Uesugi, A. Matsusue, T. Fujita, S. Takagi, T. Hatta, A. Sugitatsu, and H. Watanabe, "Cost-Effective 10.7 Gbit/s Cooled TOSA Employing Rectangular TO-CAN Package Operating up to 90°C," Optical Fiber Communication Conference (OFC) 2010, JWA38, San Diego, CA, USA, March, 2010.
[15] http://crosslight.com/
[16] D. Zhou, R. Zhang, H. Wang, B. Wang, J. Bian, X. An, L. Zhao, H. Zhu, C. Ji, and W. Wang, "The effect of zinc diffuction on extinction ratio of MQW electroabsorption modulator integrated with DFB laser," SPIE Photonics Asia, vol.9267, 926714-1, Beijin, China, 2014.
[17] U. Gösele and F. Morehead, "Diffusion of zinc in gallium arsenide: A new model," J. Appl. Phys., vol.52, no.7, pp.4617–4619, 1981.
[18] N. Otsuka, M. Kito, M. Ishino, and Y. Matsui, "Control of double diffusion front unintentionally penetrated from a Zn doped InP layer during metalorganic vapor phase epitaxy," Journal of Applied Physics, vol.84, no.8, pp.4239–4247, 1998.
[19] T. Yamanaka, H. Fukano, K. Tsuzuki, M. Tamura, R. Iga, M. Ogasawara, Y. Kondo, and T. Saitoh, "Influence of Zn diffusion on bandwidth and extinction in MQW electroabsorption modulators buried with semi-insulating InP," Proc. OECC2003, pp.439–440, Shanghai, P.R.China, 2003.
[20] W. Kobayashi, N. Fujiwara, T. Shindo, Y. Ohiso, T. Yoshimatsu, S. Kanazawa, T. Ohno, K. Hasebe, H. Ishii, and H. Matsuzaki, "Low-power consumption 28-Gb/s 80-km transmission with 1.3-μm SOA-assisted extended-reach EADFB laser," IEEE Journal of Lightwave Technology, vol.35, no.19, pp.4297–4303, Oct. 2017.

Wataru Kobayashi received B.S. and M.E. degrees in applied physics, and a Dr. Eng. degree in nano-science and nano-engineering from Waseda University, Tokyo, Japan, in 2003, 2005 and 2011, respectively. In 2005, he joined NTT Photonics Laboratories. He is now with NTT Device Technology Laboratories, Atsugi, Kanagawa, Japan. His research interests include the development of optical semiconductor devices. He is a member of the Institute of Electronics, Information, and Communication Engineers (IEICE) and a professional engineer, Japan, P. E. Jp (Electrical & Electronics Engineering).

Shigeru Kanazawa received his B.E., M.E., and Ph.D. degrees in Electronic Engineering from the Tokyo Institute of Technology, Tokyo, Japan, in 2005, 2007 and 2016, respectively. In April 2007, he joined Nippon Telegraph and Telephone (NTT) Photonics Laboratories (now NTT Device Innovation Center), Atsugi, Kanagawa, Japan. He is engaged in research and development of optical semiconductor devices and integrated devices for optical communications systems. Dr. Kanazawa is a senior member of the IEEE/Photonics Society and the Institute of Electronics, Information and Communication Engineers of Japan (IEICE), and a member of the Japan Society of Applied Physics (JSAP) and the Japan Institute of Electronics Packaging (JIEP).

Takahiko Shindo received his B.E., M.E., and Ph. D. degrees in Electrical and Electronic Engineering from Tokyo Institute of Technology, Japan, in 2008, 2010, and 2012, respectively. He received a research fellowship for young scientists from the Japan Society for the Promotion of Science for the years 2010 to 2012. After receiving the Ph. D. degree in 2012, he was working as a Research fellow at the Japan Society for the Promotion of Science, Japan. In April 2013, he joined Nippon Telegraph and Telephone (NTT) Photonics Laboratories (now NTT Device Technology Laboratories), NTT corporation, Atsugi-shi, Japan. He has been engaged in research on optical semiconductor devices. Dr Shindo is a member of the IEEE Photonics society, the Japan Society of Applied Physics, and the Institute of Electronics, Information and Communication Engineers of Japan.

Manabu Mitsuhara received the B.E. and M.E. in applied physics and the Dr. Eng. Degree from Osaka University, Osaka, Japan, in 1989, 1991, and 2000, respectively. In 1991, he joined NTT Optoelectronics Laboratories, Kanagawa, Japan. From 2000 to 2003, he worked for new business development in the area of e-Learning at NTT Communications Corporation, Tokyo. He is currently engaged in the growth of InP-based materials for near- and mid-infrared optoelectronic devices. He is a member of the Institute of Electronics, Information, and Communication Engineers (IEICE) and a member of the Japan Society of Applied Physics (JSAP).

Fumito Nakajima received the B.E., M.E. and Ph.D. degrees from Hokkaido University, Hokkaido, Japan, in 1998, 2000 and 2003, respectively. In 2003, he joined the NTT Photonics laboratories, Nippon Telegraph and Telephone Corporation, Kanagawa, Japan. He has been involved in research and development on high-speed photodiodes and avalanche photodiodes for optical receivers. He is currently a senior research engineer, supervisor, group leader at NTT Device Technology Laboratories, Kanagawa, Japan. Dr. Nakajima is a member of the Institute of Electronics, Information, and Communication Engineers of Japan (IEICE).